NTNU
Norwegian University of
Science and Technology

Modelling of Åsgard subsea gas compression station for condition monitoring purposes

Julie Berge Ims

December 2017

Project Thesis

Department of Chemical Engineering

Norwegian University of Science and Technology

Supervisor 1: Johannes Jäschke

Supervisor 2: Adriaen Verheyleweghen

Acknowledgment

This work has been carried out at the Norwegian University of Science and Technology at the Department of Chemical Engineering. I would like to thank my supervisors Johannes Jäschke and Adriaen Verheyleweghen for continuous assistance and feedback throughout the process. You have given me the ability to explore and investigate interesting topics and yet forced me into structuring my priorities to improve my work.

J.B.I.

Summary

This project thesis proposes an approach for integrating health monitoring, prognostics and control to achieve an economic optimal operational strategy, without compromising the reliability of the system. A detailed separator model will be implemented to provide accurate predictions of liquid carry over to the wet-gas compressor. A new separator model has been proposed to reduce uncertainty and enable enhanced production through less conservative operations. The mathematical model designed is based on a correlation between the cyclone separation efficiency and the dimensionless re-entrainment number.

Health monitoring techniques are employed to consider and evaluate the condition of the overall system. The degradation of equipment and remaining useful life (RUL) of equipment are used for condition monitoring purposes. Paris' law for crack propagation is used to predict degradation of equipment. Risk of failure in terms of cumulative hazard is used to predict RUL of equipment. Parameters in the RUL distribution are estimated based on the aging process. The expected RUL increases with decreasing degradation. That is reasonable as a smaller bearing crack-length would suggest that the system is operational for a longer time, compared to a larger crack-length. The results in terms of the economic outcome are somewhat unexpected. The operational strategy is more profitable when RUL of equipment is used to monitor the health condition development. Adjustments to the risk of failure implementation can be done to achieve a more intuitive result.

Trondheim, 2017-12-19

Julie Berge Ims

Julie Berge Ims

Contents

List of Figures

List of Tables

Nomenclature

List of symbols

N_μ	Dimensionless viscosity number.	-
α	Cyclone Separation efficiency.	-
δ_l	Liquid film thickness in the cyclone wall	m
$\dot{m}_{gas}$	Gas production rate from operation. Measured as gas exiting the compressor.	kg/s
$\dot{Q}$	Volumteric liquid flow in the cyclone wall.	m^3/s
ϵ_r	Upper bound for the reliability objective in the optimal control problem.	-
Γ	Volumteric liquid flow in the cyclone wall per unit wetted perimeter.	m^2/s
$\hat{\theta}$	Angle to indicate direction of gas flow in the wetted perimeter.	^{o}
λ_w	Scale parameter in Weibull distribution.	-
μ_l	Dynamic viscosity for liquid film on cyclone wall.	Pa/s
ϕ	Objective function in the stochastic non-linear optimization problem.	-
ϕ_e	Economic objective in the optimal control problem.	-
ϕ_r	Reliability objective in the optimal control problem.	-
ρ_g	Density of the gas in the gas stream.	kg/m^3
ρ_l	Density of the liquid film on the cyclone wall.	kg/m^3
σ	Interfacial/surface tension between two phases.	mN/m

$\tau_{i,tg}$	Tangential component of shear stress acting on the film due to the gas flow.	Pa
$\tau_{w,tg}$	Tangential component of shear stress acting on the wall due to the liquid film.	Pa
A	Non-anticipativity constraints in the stochastic non-linear optimization problem.	-
p	Stochastic parameters in the stochastic non-linear optimization problem.	-
u	Vector with inputs in the stochastic non-linear optimization problem.	-
x	Vector with algebraic and differential states in the stochastic non-linear optimization problem.	-
θ	Angle between vertical and tangential gas velocity on the cyclone wall.	^{o}
A	Constant for linear model.	-
a	Model-constant.	-
a_l	Centrifugal acceleration acting on the liquid film in the cyclone wall.	m/s^2
B	Constant for linear model.	-
c_{Paris}	Lumped parameter in Paris' law for crack propagation.	-
$cost(t)$	Cost from production.	-
D	Separator diameter.	m
E	Dimensionless Re-entrainment number.	-
f	Inequality constraints in the stochastic non-linear optimization problem.	-
F_d	Drag force from the gas flow on the liquid wave peak.	N
F_σ	Retaining force of the surface tension.	N
$f_{g,i}$	Friction factor for gas on the liquid film.	-
$f_{i,w}$	Friction factor for liquid on the cyclone wall.	-
F_{RUL}	Cumulative distribution function for RUL.	-
f_{RUL}	Probability density function for RUL.	-
g	Equality constraints in the stochastic non-linear optimization problem.	-

h	Bearing crack length in the wet-gas compressor.	mm
H_{RUL}	Conditional probability distribution, cumulative hazard function.	-
h_{RUL}	Conditional probability function, hazard function.	-
i	Discount rate for Net present value calculations.	-
K	Constant.	-
k	Variable used to track time step in the stochastic non-linear optimization problem.	-
k_w	Shape parameter in Weibull distribution.	-
m	Constant.	-
N	Number of time periods. It is the length of the horizon in the stochastic non-linear optimization problem.	-
P	Motor power in the wet-gas compressor.	Watt
p_i	Probability of occurrence for scenario i in the stochastic non-linear optimization problem.	-
P_w	Wetted perimeter	m
P_{out}	Pressure downstream from the choke.	bar
$R_{RUL}(t)$	Reliability of a component or a system.	-
Re_l	Reynolds number for liquid film on the cyclone wall.	-
S	Number of scenarios in the stochastic non-linear optimization problem.	-
Srg	Surge condition for compressor choking.	-
Stw	Stonewall condition for compressor choking.	-
T	Motor Torque in the wet-gas compressor.	Nm
t	Time variable.	Years
t_f	Inital time until the next maintenance intervention.	Years
u_l	Velocity of the liquid film on the cyclone wall.	m/s

u_z	Vertical gas velocity on the cyclone wall.	m/s
u_{choke}	Choke opening as input to the system.	-
u_{comp}	Compressor speed as input to the system.	Hz
$u_{g,s}$	Superficial gas velocity in the separator unit.	m/s
$u_{l,tg}$	Tangential velocity of the liquid film on the cyclone wall.	m/s
x	Differential states in the optimization problem.	-
x_0	Initial conditions for equality constraints.	-
z	Algebraic states in the optimization problem.	-

List of abbreviations

AFC	Axial Flow Cyclone
CDF	Cumulative distribution function
DAE	Differential algebraic equation
GVF	Gas volume fraction
MPC	Model predictive control
NLP	Non-linear problem
NPV	Net Present Value
OCP	Optimal control problem
PHM	Prognosis and Health Monitoring
RUL	Remaining useful life
PDF	Probability density function

Chapter 1

Introduction

Subsea processing technology is developed to overcome many challenges associated with topside oil and gas operations. This technology enables oil and gas production from reservoirs and fields previously deemed too remote. The main objective with subsea processing systems is to strengthen the economic result from the operation through cost reduction and increase in production. However, new challenges arise when operating oil and gas systems on the seabed. Safe and efficient operation of subsea processing systems imposes strict requirements both with respect to equipment design and reliability, in order to avoid unplanned shutdowns and expensive maintenance engagements.

This project thesis focuses on the subsea gas compression station at the Åsgard field, as depicted in Figure 1.1. A detailed separator model is proposed in order to accurately predict liquid carry over to a wet-gas compressor. The model enables a reduction in uncertainty and the possibility to operate the system in a less conservative way. Health monitoring techniques are employed to consider and evaluate the condition of the overall system[22].

Figure 1.1: Artist rendition of the Åsgard gas compression station. Copyright: Aker Solutions.

1.1 Motivation

The objective of this project thesis is to develop a separator model for the subsea gas compression station at the Åsgard field, and to propose health degradation models to be used to obtain an optimal operational strategy. A detailed separator model with axial flow cyclones is proposed to better mimic the separator patented by Statoil for the Åsgard subsea gas compression station.

The purpose of the new separator model is to be able to accurately predict liquid carry over to a wet-gas compressor. The bearings in the wet-gas compressor are prone to damage when, among other things, liquid droplets cause mechanical stress on compressor blades with high rotational speed. The bearings are considered to be vital in the operation, and should be replaced immediately if broken. Health monitoring is employed to evaluate and predict the condition of the overall system [22]. In the context of this work, the condition will be estimated in terms of bearing crack-length in the wet-gas compressor and as remaining useful life (RUL) of the equipment. This project thesis will propose an approach for integrating health state prognostics in order to obtain a strategy that ensures economic optimal operation, without jeopardizing the reliability of the subsea system.

1.2 Approach

The study is based on a mathematical model of the Åsgard subsea gas compression station. The original model is implemented in MATLAB by supervisor Adriaen Verheyleweghen. The implementation is based on a model predictive control-like framework to include prognostics and health monitoring information in the optimization routine. A new separator model has been implemented and adapted to the original system. Algebraic and differential equations has been added to enable remaining useful life of equipment calculations for condition monitoring purposes. The data used is not original data from the Åsgard subsea gas compression station, but fictional data intended for optimization and modelling purposes.

Chapter 2

Theory

This chapter gives a brief description of the subsea gas compression station in the Åsgard field. Supporting theory for the development of the separator model and the compressor degradation model will also be given here. The chapter includes a description of health prognostics models used for optimization purposes in a model predictive control framework.

2.1 Process description

The subsea gas compression station at the Åsgard field is the very first compressor to be installed and operated on the seabed. It is considered to be pioneering compression technology [18]. The purpose of the gas compression station at the Åsgard field is to boost the pressure of the reservoir stream such that it will overcome pressure drop in transportation pipes to topside facilities. However, the maturity level of the technology is limited for multiphase [22]. Hence, the liquid and gas components are separated to allow an increase in pressure. The system is illustrated in Figure 2.1. It consists of a well choke that controls the reservoir stream entering the gas compression station. A separator downstream from the well choke separates gas from liquid. Incomplete separation causes liquid droplets to exit the separator with the gas through the gas outlet. The liquid pressure is subsequently boosted by a pump and the gas pressure is increased in a wet-gas compressor [22].

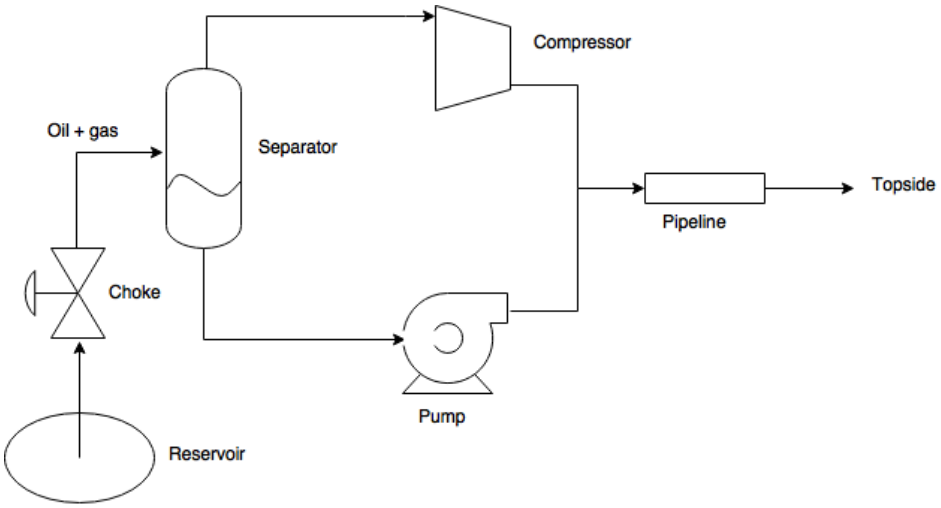

Figure 2.1: Process diagram of the subsea gas compression station in the Åsgard field [22].

2.2 General description of framework

The subsea system at the Åsgard field can be defined by a set of algebraic and differential states as well as control inputs. A dynamic model and current measurements can be used to predict future states of the system. A model predictive control (MPC) framework utilizes current measurements and predictions of future values of the output to obtain an optimal operational strategy for the subsea system [17]. Accurate model predictions can provide valuable information of the system degradation,which can be used to avoid unplanned break-downs for the subsea plant. Essentially, the accuracy of the process model affects the success of the MPC [17].

2.3 Model description

This section will describe the model used for this work. It is assumed that the fluid can be described as liquid and gas. The thermodynamics of the model is ignored. The separator model and the model for the degradation of the bearings in the wet-gas compressor are introduced in this section. Models for the compressor and the choke is not discussed here. The interested reader is referred to [22] for compressor and choke models. The pipeline and the pump are not modeled, but will be included in future work.

2.3.1 Separator model

The separator developed for the subsea gas compression station at the Åsgard field is based on a Statoil patented separator for liquid-gas separation of an inlet flow which predominantly contains gas. This is a

separation unit with spinlet inlet configuration and axial flow cyclones [2]. It is developed to be able to separate the last liquid droplets from a gas flow, both at high flow rates and high pressure [6].

The separator is a vertical standing container with an inlet for the liquid-gas flow and outlets for gas- and liquid flows. The inlet is a spinlet arrangement for flow distribution to receive and make the flow move in rotational movements around the vertical axis of the main container towards a porous pipe configuration. This porous pipe component is equipped to handle the total inlet flow and drives the flow towards the gas outlet. The inside of the porous tubular wall has a smooth surface so that no liquid can be deposited. The porous tubular body have open porosity towards the inner wall so that the tubular wall is permeable for fluid. Approximately 80% of the gas stream will flow vertically through the porous tubular body and towards the gas outlet. The remaining 20% will flow horizontally through the wall of the porous tubular body and into an annular space between the tubular component and the container wall. Here, droplets will move downwards to the liquid outlet and gas will move upwards to the gas outlet.
The separator may contain a wired mesh demister in the gas outlet between the container wall and the upper end of the tubular wall [6]. An illustration of a separator with wired mesh pads is shown in Figure 2.2. However, due to the maturity level of the technology, mesh pads are currently not considered an option for subsea processing systems due to the risk of clogging [18]. Hence, it is assumed that demisters are not utilized in the Åsgard subsea gas compression station.

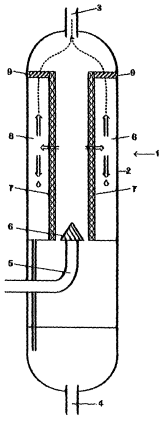

Figure 2.2: Illustration of a separator unit (with mesh pads) patented by Statoil[6].

Statoil released an illustration of separation efficiency as a function of superficial gas velocity for their new separation device compared with a typical axial flow cyclone separator. Figure 2.3 indicates that the Statoil patented separator device has better separation performance compared to generic axial flow cy-

clones. Note that this is the performance of a separator unit with a mesh pad. It is therefore reasonable to believe that the effective separation efficiency of the Åsgard separator would be somewhat lower.

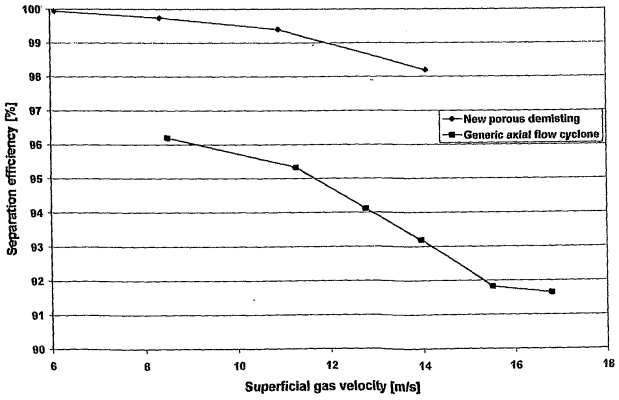

Figure 4 Comparison of generic axial flow cyclone and new porous demisting at liquid load of 0.022 – 0.030 vol%.

Figure 2.3: Separator efficiency plotted against Superficial gas velocity for the Statoil patented separator device and a generic axial flow cyclone [6].

Axial flow cyclone

The Statoil patented separator consists of a spinlet configuration and axial flow cyclones. This project thesis will make a rough approximation and create a separator model containing axial flow cyclones only. A cyclone separator, also called centrifugal separator, acts by making the fluid move in rotational movements in order for the centripetal forces to separate light and heavy components in the fluid. The fluid is likely to follow a helical path where heavier components will accumulate at the outer peripheral of the helical trail, while lighter components will gather in the center along the vertical axis. Gravitational forces will also contribute to separate heavier components, whereas lighter components may rise towards the gas outlet [6].

There are multiple well developed models for axial flow cyclones. In this particular case, it is essential to develop a detailed separator model to be able to accurately predict liquid carry over. A detailed model reduces uncertainty and provides opportunity to shift constraints in the optimal control problem (OCP). Shifting constraints can make the operation less conservative and thus more profitable. In terms of subsea operating conditions, the separator model must also be able to handle higher pressure and higher flow rates.

A steady state model was developed by [3] for a scrubber with a mesh pad used for primary separation and axial flow cyclones for separating the last droplets from the gas stream. In view of the risk of clogging for subsea processing systems, this report will only concentrate on the axial flow cyclone section of the steady state model. A mathematical model based on flow development, fluid properties and cyclone geometry has been developed to correlate the dimensionless re-entrainment number and separation efficiency in a cyclone [3]. This mathematical correlation has been fundamental in this particular separator model.

Re-entrainment number

The performance degradation of the axial flow cyclone used in this study [3] was governed by some type of re-entrainment mechanism, i.e. not insufficient separation of small droplets. The separation efficiency is dominated by the re-entrainment of liquid which has settled on the separator wall. Various mechanisms for re-entrainment of liquid into a gas stream has been described [3]. Figure 2.4 illustrates the re-entrainment mechanisms "Roll wave" and "Wave undercut". The "Roll wave" mechanism is asso-

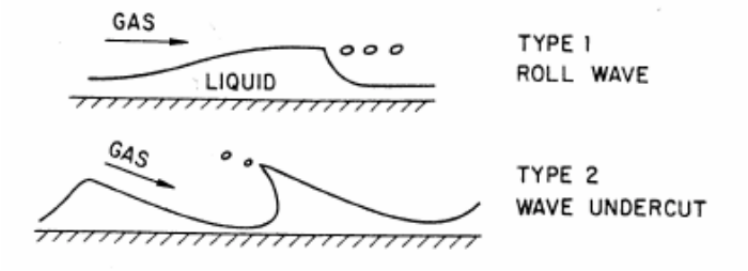

Figure 2.4: Re-entrainment mechanisms in the AFC [3].

ciated with droplets that are cut of a roll-wave peak. This is the dominant mechanism in liquid film with high Reynolds number and in the transition regime. The "Wave undercut" mechanism is connected to cutting a wave peak. This is a governing mechanism in liquid film with relatively low Reynolds number. In the context of this study, it assumed that liquid film on the cyclone wall is in the transition regime. Calculations of Reynolds number for the liquid film on cyclone wall will justify this assumption. A force balance was applied as a criterion for the eruption of re-entrainment. The retaining force, F_σ, of the surface tension, σ, between the two phases was evaluated with the drag force from the gas flow on the liquid wave peak, F_d. Roll wave re-entrainment was presumed to be feasible if the drag force acting on the wave top exceeded the retaining force [3]:

$$F_d \geq F_\sigma. \tag{2.1}$$

The criterion for the transition regime was expressed as:

$$\frac{\mu_l \, u_{g,s}}{\sigma}\sqrt{\frac{\rho_g}{\rho_l}} \geq 11.78 N_\mu^{0.8} \, Re_l^{-1/3} \quad \text{for } N_\mu \geq \frac{1}{15} \tag{2.2}$$

$$\frac{\mu_l \, u_{g,s}}{\sigma}\sqrt{\frac{\rho_g}{\rho_l}} \geq 1.35 Re_l^{-1/3} \quad \text{for } N_\mu \leq \frac{1}{15}. \tag{2.3}$$

The outburst of such re-entrainment mechanism from Equation 2.3, depends on the Reynolds number of the liquid film, Re_L, on the cyclone wall . It is assumed that liquid carry-over is a constant fraction of entrained liquid. Thus the liquid flow, $\dot{Q}_l$, on the cyclone wall must be corrected for this [3]. Hence, the expression for the Reynolds number, Re_L for the liquid film on the cyclone wall results in:

$$Re_L = \frac{\rho_l \, u_l \delta_l}{\mu_l} = \frac{\rho_l \, \Gamma}{\mu_l} = \frac{\rho_l \, \dot{Q}_l \, \alpha}{\mu_l \, \mathrm{P}_w}. \tag{2.4}$$

Neither the liquid film thickness, δ_l, nor the liquid film velocity, u_l, are known at this stage. The product of the two quantities, Γ, is the volumetric liquid flow, $\dot{Q}_l$, per unit wetted perimeter, P_w. ($\dot{Q}_l \alpha$) is the corrected volumetric liquid flow. α is here the separation efficiency in the AFC. ρ_l is the density and μ_l denotes the viscosity of the liquid film. The wetted perimeter of the cyclone, P_w, must take into account the direction of the gas flow [3]. If the cyclone body is flattened to a rectangle, the circumference in the container is the length of the short side as depicted in Figure 2.5.

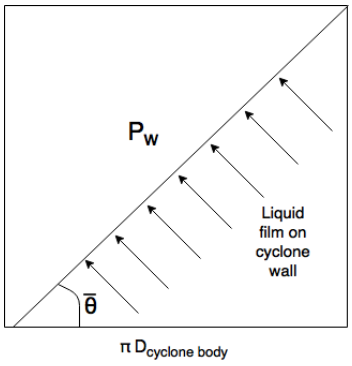

Figure 2.5: The lower section of the cyclone when it is flattened. The wetted perimeter of the cyclone is marked as the diagonal in the figure [3].

The angle, $\hat{\theta}$, is used to indicate the direction of the gas flow. The relative angle to the swirl is assumed to be approximately $\hat{\theta} = 45°$. D is the diameter of the cyclone. The wetted perimeter can be defined with this equation:

$$\mathrm{P}_w = \frac{\pi \, D}{\cos\hat{\theta}}. \tag{2.5}$$

The force balance in equation 2.1 accounts for changes in shear stress acting on the liquid wave due to the drag force from the gas flow through the dimensionless viscosity number, N_μ. This parameter is used to analyze the viscous force induced by internal flow. The viscosity number is defined through the following relation:

$$N_\mu = \frac{\mu_l}{\sqrt{\rho_l \, \sigma \, \sqrt{\frac{\sigma}{a_l \, \Delta\rho}}}}. \tag{2.6}$$

σ is the interfacial tension between the liquid and the gas phase. $\Delta\rho = \rho_l - \rho_g$ and a_l is the centrifugal acceleration acting on the liquid film:

$$a_l = \frac{2 \, u_{l,tg}^2}{D}, \tag{2.7}$$

where the tangential velocity component of the liquid film, $u_{l,tg}$, is unknown at this stage. The tangential components of the shear stress acting on the wall due to the liquid film and on the liquid film due to the gas are $\tau_{w,tg}$ and $\tau_{i,tg}$, respectively. The tangential shear stresses are defined as:

$$\tau_{i,tg} = f_{g,i} \frac{\rho_g \, u_{r,tg}^2}{2} \tag{2.8}$$

$$\tau_{w,tg} = f_{l,w} \frac{\rho_l \, u_{l,tg}^2}{2} = \tau_{i,tg}. \tag{2.9}$$

Assumptions about the gas velocity relative to the liquid film velocity are defined as:

$$u_{g,tg} >> u_{l,tg} \Rightarrow u_{r,tg} \approx u_{g,tg}. \tag{2.10}$$

Based on these assumptions the tangential liquid velocity can be expressed as:

$$u_{l,tg} = \sqrt{\frac{f_{g,i} \, \rho_g \, u_{g,tg}^2}{f_{l,w} \, \rho_l}}. \tag{2.11}$$

ρ_g is the gas density. $u_{g,tg}$ is the tangential gas velocity which will be discussed later. The f's are friction factors which has not yet been measured for liquid flow on a cyclone wall. However, friction factors developed for annular flow in pipes were used by [3] and the same approximation is done in this report as well. $f_{g,i}$ is the friction factor for gas on the liquid film and is expressed through the following relation:

$$f_{g,i} = 0.005\left[1 + 300\frac{2\delta_l}{D}\right]. \tag{2.12}$$

$f_{g,i}$ is the friction factor for liquid on the wall and is expressed as:

$$f_{i,w} = \left(K \cdot Re_L^m\right)^2. \tag{2.13}$$

$K = 3.73$ and $m = -0.47$ for $2 < Re_L < 100$. $K = 1.962$ and $m = -1/3$ for $100 < Re_L < 1000$. Note that this study will assume that the liquid film on the cyclone wall is in the transition regime. The friction factors depend on the thickness of the liquid film, δ_l, on the cyclone wall. Liquid film thickness, δ_l, can be found from Equation 2.4:

$$\Gamma = \frac{\dot{Q}}{P_w} = u_l\,\delta_l \quad \Rightarrow \delta_l = \frac{\dot{Q}_l}{P_w\,u_l}, \tag{2.14}$$

where liquid film velocity can be expressed as

$$u_l = \frac{u_{l,tg}}{cos(\hat{\theta})}. \tag{2.15}$$

The expression for the liquid film thickness, δ_l, can thus be simplified based on Equation 2.5, 2.14 and 2.15:

$$\delta_l = \frac{\dot{Q}_l}{\pi\,D\,u_{l,tg}}\cos^2\hat{\theta}. \tag{2.16}$$

The tangential gas velocity, $u_{g,tg}$, increases with radius, similar to a solid body rotation. The gas viscosity is low relative to the liquid. Hence, the velocity profile for the tangential gas velocity close to the cyclone wall will resemble a loss-free-vortex profile [3]. The tangential gas velocity in the cyclone can therefore be considered as something between a loss-free vortex and a solid body rotation. However, the gas velocity at the liquid-gas interface on the cyclone wall is more important for re-entrainment analyzes. The wall gas velocity is illustrated in Figure 2.6.

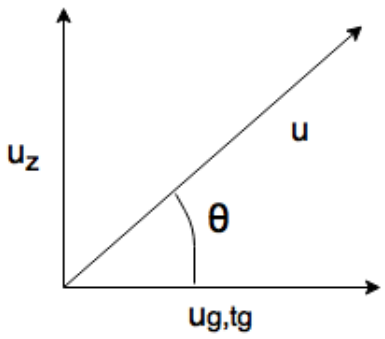

Figure 2.6: Flow coordinates at the cyclone wall [3].

The tangential gas velocity profile changes along the vertical axis, but some simplifying approximations

can be done. The superficial gas velocity, $u_{g,s}$, is assumed to be a factor 0.8 less than the vertical gas velocity, u_z, close to the cyclone wall in the middle section of the cyclone [3].

$$u_{g,s} = 0.8\ \left(u_z\right) = 0.8\ \left(u_{g,tg} \cdot \tan(\theta)\right). \tag{2.17}$$

Based on all these expressions, a dimensionless re-entrainment number, E, was developed to characterize the cyclone separation efficiency, α, where the separation is governed by re-entrainment:

$$E(\alpha, u_{l,tg}, a) = \frac{\frac{\mu_l\ u_{g,s}}{\sigma}\left(\frac{\rho_g}{\rho_l}\right)^{0.8}}{N_\mu^a\ Re_l^{-1/3}}. \tag{2.18}$$

Excellent correlation between the cyclone separation efficiency and the dimensionless re-entrainment number may indicate that the separation efficiency is governed by liquid re-entrainment, not insufficient separation of smaller droplets. The correlation between the cyclone separation efficiency and the dimensionless re-entrainment number is expressed in the next equation:

$$\alpha = A \cdot E(\alpha, u_{l,tg}, a)\ +\ B. \tag{2.19}$$

a is a constant used to fit the re-entrainment number with the separation efficiency. It proved to be appropriate with $a = 0.4$ for this model. A and B are constants for the linear model.

2.3.2 Compressor bearing degradation model

An important aspect of subsea processing is to ensure safe operation until the next maintenance engagement. The time horizon is multiple years as frequent maintenance can become very costly. The dynamics of pressures, temperatures and flows are assumed to be instantaneous over this time period. Hence, the only dynamics of interest is the wet-gas compressor bearing degradation model [22]. The compressor bearings will degrade according to Paris' law of crack propagation. Paris' crack propagation model is commonly used for surface defects [14]. This model states that the crack length, h, will develop according to the following relation:

$$\frac{dh}{dn_{cycles}}\ =\ D \cdot (\Delta K)^n, \tag{2.20}$$

where n is an exponent, n_{cycles} is the number of cycles, D is a material constant and ΔK denotes the range of strain. This can be reformulated into a model for the development of a bearing crack length

$$\frac{dh}{dt} = h \cdot c_{Paris} \left(T^2 \cdot u_{comp}\right) = h \cdot c_{Paris} \cdot \left(\frac{P^2}{u_{comp}}\right), \tag{2.21}$$

where it is assumed that the torque, T, can be used as health indicator for gross strain [4]. c_{Paris} is a lumped parameter and is estimated from past values. P is the motor power [20].

2.4 Diagnostics and prognostics

Safe and efficient operation of subsea processing systems imposes strict requirements to equipment reliability in order to avoid unplanned shut-downs and expensive maintenance engagements. Health monitoring techniques are employed to consider and evaluate the condition of the overall system in real-time. Health degradation models for the system will be included in the optimization procedure, resulting in a model model predictive (MPC)-like framework [22]. Specifically, health diagnostics and prognostics will be integrated as the optimal operational strategy for the subsea system is being found.

Diagnostics deals with the discovery and surveillance of faults and hazards in a system. Failure can be any kind of unavailability of the system. Unavailability can be interpreted as the degree to which a system or component is not operational and accessible when required for use [8]. Prognostics on the other hand deals with the ability to anticipate health development and estimate the RUL of the system [20]. This particular system is complex with a large number of components for which diagnostics and prognostics can be challenging. Condition monitoring systems ought to be able to detect various faults. Different methods exist to monitor subsea plants. In order to limit the scope of this project thesis, a simplifying assumption has been made that only the most vulnerable components in the system are considered. The bearings in the wet-gas compressor are considered to be vital in the operation, and should be replaced immediately if broken. The bearings are prone to faults as they have multiple moving parts and a complex mechanical setup [20]. Hence, a detailed separator model is important in order to be able to accurately predict liquid carry over that are causing faults in the wet-gas compressor. This will reduce uncertainty and enables more precise health estimations. System failures which are independent of operational decisions will be neglected. This should however be addressed in future analysis.

A wide range of prognostics models are available for condition monitoring. In the context of this study,

propagation models for degradation of equipment and remaining useful life (RUL) of equipment are used for condition monitoring purposes. Paris' crack propagation model in Equation 2.21 will be used to estimate the degradation of the bearing crack-length [14]. The risk of failure captured by the cumulative hazard, will be used to constrain the RUL of equipment for the system. The latter method will be discussed in detail in the following section.

2.4.1 System reliability and remaining useful life

There exists various definitions of the term reliability. The most widely accepted definition is that reliability is the probability that a part or unit will be operational for a particular time period under specified operating conditions without failure [8]. Reliability can thus be formulated in terms of unavailability, Reliability = 1 - P(Failure), where P is the probability operator. In the context of this work, unavailability can be expressed as loss of production which is when remaining useful life (RUL) of equipment is shorter than the time until the next maintenance engagement (t_f), RUL < t_f. The probability that the component survives until the next maintenance intervention at t= t_f is called the reliability $R(t_f)$ of the component

$$\begin{aligned} R_{RUL}(t_f) &= P(RUL > t_f) = 1 - P(RUL \leq t_f) \\ &= 1 - F_{RUL}(t_f) = 1 - \int_0^{t_f} f_{RUL}(t)\, dt \\ &= \int_{t_f}^{\infty} f_{RUL}(t)\, dt. \end{aligned} \tag{2.22}$$

f_{RUL} is the probability density function (PDF) of RUL and t is the time (which is assumed to start from t = 0). A commonly used PDF for RUL of equipment is the Weibull distribution formulated as [10]

$$f_{RUL}(t) = \lim_{dt \to 0} \frac{P\,(t \leq RUL < t + dt\,)}{dt} = \begin{cases} \frac{k_w}{\lambda_w}\left(\frac{t}{\lambda_w}\right)^{(k_w-1)} e^{-\left(\frac{t}{\lambda_w}\right)^{k_w}} & t \leq 0 \\ 0 & t > 0, \end{cases} \tag{2.23}$$

where $k_w = k_w(h)$ is the shape parameter and $\lambda_w = \lambda_w(h)$ is the scale parameter [9]. It is assumed that the shape and scale-parameters depend on degradation of equipment, h [19]:

$$k_w(h) = k_a + k_b \cdot h \tag{2.24}$$

$$\lambda_w(h) = \lambda_a + \lambda_b \cdot h. \tag{2.25}$$

Note that degradation of equipment is a function of inputs, $h = h(u)$. F_{RUL} is the cumulative distribution function (CDF) of RUL which represents the probability of having a system breakdown before $t = t_f$.

$$F_{RUL}(t_f) = P\,(\,RUL \leq t_f\,) = \int_0^{t_f} f_{RUL}(t)\,dt. \tag{2.26}$$

More specific, F_{RUL} feature the unconditional probability that the system will fail before $t = t_f$. In the context of this study, it is more convenient to deal with failure before t_f, given survival up to time t [19]. Assuming no failures have occurred up to time t, the conditional probability expression can be:

$$P\,(t \leq RUL < t + dt\,|RUL \geq t) = \frac{P\,(t \leq RUL < t + dt\,)}{P(RUL \geq t)} \tag{2.27}$$

The conditional probability gives rise to a conditional probability function commonly called the hazard function. The hazard function is the conditional failure rate and is denoted $h_{RUL}(t)$ [10].

$$\begin{aligned} h_{RUL}(t) &= \lim_{dt \to 0} \frac{P\,(t \leq RUL < t + dt\,|RUL \geq t)}{dt} \\ &= \lim_{dt \to 0} \frac{P(t \leq RUL < t + dt\,)}{P(RUL \geq t)\,dt} \\ &= \frac{f_{RUL}(t)}{R_{RUL}(t)} = \frac{f_{RUL}(t)}{1 - F_{RUL}(t)}. \end{aligned} \tag{2.28}$$

h_{RUL} is not a probability distribution, but a risk of not surviving until next maintenance (t_f) at time t, given that the system has survived up to time t. Then the risk of not surviving associated with all parts of the production from t = 0 to t = t_f is defined in the cumulative risk [19]:

$$H_{RUL}(t_f) = \int_0^{t_f} h_{RUL}\,dt. \tag{2.29}$$

The risk of failure is captured by the cumulative hazard, which will be constrained in order to limit the RUL of equipment.

2.5 Model Predictive Control

Unplanned shutdowns and frequent maintenance interventions can become very costly when operating on the seabed. Information about the degradation of system components can be used to make effective maintenance policies. This information can be used to forecast the health condition of system components in the future. Prognosis and Health Monitoring (PHM) techniques can be used to detect faults and

predict whether the subsea system can operate safely until the next planned maintenance. Predictions of the remaining useful life (RUL) of equipment can provide valuable information used to schedule the next maintenance intervention[15].

This project thesis proposes a model predictive control (MPC) framework by including PHM information in the optimization routine. Essentially the model predictive control philosophy is based on optimization of future inputs. Figure 2.7 illustrates how a the most recent measurement of the actual plant uses the process model to predict future states. An open-loop optimization is done to predict optimal control inputs for a particular prediction horizon, N. The first control input is implemented before this process is repeated [21].

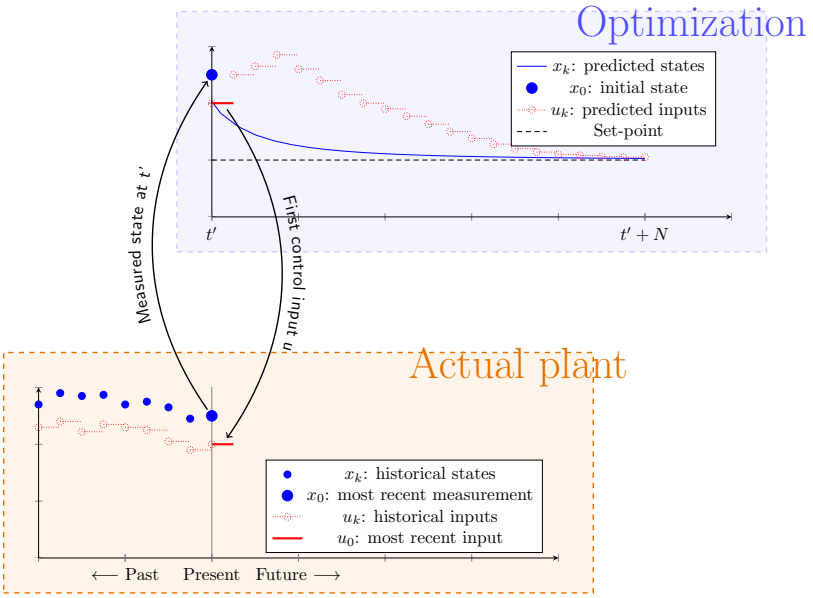

Figure 2.7: Illustration of the sequence of events in a model predictive controller [21].

In the context of this work, a shrinking time horizon will be used by decreasing the prediction horizon by one time step. However, this project thesis will only discuss open-loop optimization with initial time horizon, t_f, for the subsea system. Hence, the optimal control problem (OCP) solved for the open-loop

optimization can be formulated as follows:

$$\begin{aligned} \min_{x,u,z} \quad & \int_o^{t_f} \phi(\mathbf{x},\mathbf{z},\mathbf{u},\mathbf{p}dt \\ \text{s.t.} \quad & f(\mathbf{x},\mathbf{z},\mathbf{u},\mathbf{p}) = \frac{dx}{dt} \\ & g(\mathbf{x},\mathbf{u},\mathbf{z},\mathbf{p}) = 0 \\ & \mathbf{x}_L \leq \mathbf{x} \leq \mathbf{x}_u \\ & \mathbf{z}_L \leq \mathbf{z} \leq \mathbf{z}_u \\ & \mathbf{u}_L \leq \mathbf{u} \leq \mathbf{u}_u \end{aligned} \tag{2.30}$$

In this set of equations, $\mathbf{x}$ denotes the algebraic states and $\mathbf{z}$ denotes the differential states. $\mathbf{u}$ denotes is the inputs and $\mathbf{p}$ are the stochastic parameters. g is the equality constraints and and f is the inequality constraints. ϕ is the objective function. The algebraic and differential states as well as the inputs, have upper and lower bounds. In the context of this work, the controller aims to prevent system breakdown before the scheduled maintenance at time $t = t_f$. Hence, constraints will be imposed on system degradation and RUL of equipment to ensure that accumulated degradation level will stay below a safety threshold at the end of the time horizon[15]. In future work, the sequence of optimal control inputs in the open-loop optimization is combined with a closed-loop method in the MPC.

2.6 Non-linear optimization under uncertainty

Model Predictive Control (MPC) is a control scheme that uses a model of the plant to obtain an optimal control strategy. However, a downside to this is that stability and performance of the MPC depends on the precision of the model. A stochastic optimization-based system can be applied for predictive control subject to uncertainty [12]. This will give rise to a stochastic non-linear optimization problem which can be expressed as [20]:

$$\begin{aligned} \min_{\mathbf{x}_k,\mathbf{u}_k} \quad & \sum_{k=1}^{N} \quad (\phi(\mathbf{x}_k,\mathbf{u}_k,\mathbf{p})) \\ \text{s.t.} \quad & f(\mathbf{x}_k,\mathbf{u}_k,\mathbf{p}) \leq 0 \quad \forall k = 1....N \\ & g(\mathbf{x}_k,\mathbf{u}_k,\mathbf{p}) = 0 \quad \forall k = 1....N. \end{aligned} \tag{2.31}$$

In this set of equations, $\mathbf{x}$ denotes both algebraic and differential states, $\mathbf{u}$ denotes the inputs and $\mathbf{p}$ are the stochastic parameters. N is the length of the horizon and ϕ is the objective function. g is the equality constraints and and f is the inequality constraints. k denotes the time steps. A stochastic problem for-

mulation is considered to ensure robustness against disturbance and uncertainty in the system model. Hence, a robust non-linear MPC scheme with a scenario-based approach to uncertainty is necessary to embed parameter uncertainty in the optimization problem. A scenario-based approach to uncertainty will convert the uncertain parameter distribution to discrete values by having a finite number of parameter realizations [12][7]. A scenario is a combination of different parameter realizations with associated probability of occurrence as illustrated in Figure 2.8. The scenario will act as a path from the root to leaf of the scenario tree [20].

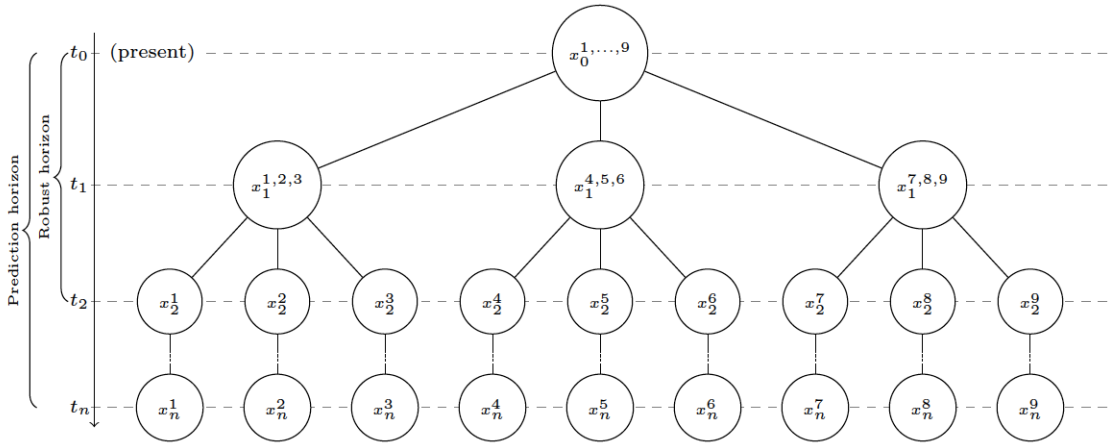

Figure 2.8: Scenario tree with robust horizon $N_R = 2$, prediction horizon $N = n$ and number of scenarios S = 9 [21].

The deterministic equivalent of the stochastic non-linear problem can be expressed as

$$\begin{aligned} \min_{\mathbf{x}_{l,k},\mathbf{u}_{l,k}} \quad & \sum_{l=1}^{S} p_i \sum_{k=1}^{N} (\phi(\mathbf{x}_{l,k},\mathbf{u}_{l,k})) \\ \text{s.t.} \quad & f(\mathbf{x}_{l,k},\mathbf{u}_{l,k}) \leq 0 \quad \forall l = 1....S\,, k = 1...N \\ & g(\mathbf{x}_{l,k},\mathbf{u}_{l,k}) = 0 \quad \forall l = 1....S\,, k = 1...N \\ & \sum_{l=1}^{S} \mathbf{A}_{l,k}\mathbf{u}_{l,k} = 0 \;\; \forall k = 1....N, \end{aligned} \tag{2.32}$$

where S is the number of scenarios and p_i is the probability of occurrence for scenario i. $\mathbf{A}$ are the non-anticipativity constraints, which are imposed such that decisions at the nodes in the scenario tree which are based on the same information are equal [12].

It is rather difficult to create a scenario tree that captures all aspects of the uncertainty in the system. However, it is preferable to create the tree as small as possible due to the complexity of the non-linear

optimization problem. The size of the optimization problem will grow exponentially with the number of uncertainties evaluated and the prediction horizon (number of stages, N). A robust horizon, N_R is introduced to limit the problem by branching the tree until a certain stage [12]. Then, the uncertainty is assumed to be constant until the end of the prediction horizon. In the context of this work, the scenario tree is generated using combinations of minimum, maximum and expected uncertain parameter realization [12]. In this project thesis two parameters are considered uncertain: the c_{Paris} parameter in the crack propagation model and the gas volume fraction in the reservoir, GVF [20]. For simplicity, GVF is approximated to be at its expected value throughout this study which results in only one uncertain parameter, c_{Paris}. The possible realizations of the uncertain parameter are given in Table 2.1.

Table 2.1: Variable realizations of the uncertain parameters c_{Paris} [22].

Parameters	Low	Medium	High
c_{Paris}	0.9	1.0	1.1

2.7 Objectives

In context of this study, the main target with this subsea system is to improve the economic outcome from the operation through cost reduction and increase in production. However, safe and efficient operation imposes stringent requirements with respect to equipment reliability. Hence, the ultimate objective is twofold:

1. Prevent premature failure of the subsea system.
2. Maximize net profit from operation

This results in a multi-objective optimization problem which can be formulated as:

$$\begin{aligned} \min_{u} \quad & (\phi_r(\mathbf{x},\mathbf{z},\mathbf{u},\mathbf{p}),\phi_e(\mathbf{x},\mathbf{z},\mathbf{u},\mathbf{p})) \\ \text{s.t.} \quad & \mathbf{x} \in \mathbf{X} \\ & \mathbf{u} \in \mathbf{U}. \end{aligned} \tag{2.33}$$

$\mathbf{x}$ denotes the differential states, $\mathbf{z}$ denotes the algebraic states, $\mathbf{u}$ denotes the inputs and $\mathbf{p}$ denotes the parameters. ϕ_r is the reliability objective which aims to minimize unavailability of the subsea system. ϕ_e is the economic objective, which seeks to maximize economic profit from operation. The two objectives contradict each other, hence the problem formulation ought to be rewritten to avoid infinite number of

solutions [19]. A unique optimal solution can be obtained by transforming this into a single-objective problem formulation. The new objective problem can be formulated as:

$$\begin{aligned} \min_{u} \quad & (\phi_e(\mathbf{x},\mathbf{z},\mathbf{u},\mathbf{p})) \\ \text{s.t.} \quad & \mathbf{x} \in \mathbf{X} \\ & \mathbf{u} \in \mathbf{U} \\ & \phi_r(\mathbf{x},\mathbf{z},\mathbf{u},\mathbf{p}) \leq \epsilon_r. \end{aligned} \tag{2.34}$$

ϵ_r is upper bound for the reliability objective, ϕ_r. The economic objective can be written in the following manner [19]:

$$\phi_e(\mathbf{x},\mathbf{z},\mathbf{u},\mathbf{p}) = \mathbb{E}\Big(\int_0^{t_f} c(t)\cdot cost(\mathbf{x},\mathbf{z},\mathbf{u},\mathbf{p})\; dt\Big). \tag{2.35}$$

$\mathbb{E}$ is the expected value operator and cost(**x**,**z**,**u**,**p**) is the cost associated with the states, inputs and parameters. The profit is weighted from time t to t_f by discounting future value of money at a periodic rate of return, called the discount rate. This a way to measure profit by including present and all future discounted cash flows, called the Net Present Value (NPV). NPV is expressed in Equation 2.36, where i is the discount rate and N is the number of time periods [11]. NPV is defined as:

$$NPV(i,N) = cost(\mathbf{x},\mathbf{z},\mathbf{u},\mathbf{p}) \sum_{t=0}^{N} c(t) = cost(\mathbf{x},\mathbf{z},\mathbf{u},\mathbf{p}) \sum_{t=0}^{N} (1\; +\; i)^{-t}. \tag{2.36}$$

In the context of this study, the reliability objective, ϕ_r, can be defined in multiple manners, i.e. minimizing degradation of equipment and as minimizing unavailability of the system in terms of loss of production. Degradation of equipment can be estimated from the development of the bearing crack length in the wet-gas compressor. The unavailability of the system can be measured as remaining useful life (RUL) of equipment. A detailed description of the RUL estimation is given in Section 2.4.1

2.8 Defining the optimal control problem

The objective function aims to maximize NPV of the production which is measured in terms of the gas production rate downstream from the compressor. Therefore, the OCP can be expressed as:

$$\min_{x,z,u} \quad \int_0^{t_f} \Big(-\frac{\dot{m}_{gas}(\mathbf{x},\mathbf{z},\mathbf{u},\mathbf{p})}{(1+i)^t}\Big)\, dt. \tag{2.37}$$

This is a differential algebraic equation (DAE) system, and the optimal control problem (OCP) can be solved using various methods. The OCP can be solved numerically using a so called direct method which transforms the original OCP into a non-linear programming problem (NLP). More explicitly, the direct collocation method will be used to solve this particular OCP [5]. Further details of the direct collocation method will not be discussed here. The OCP is implemented in MATLAB using the open-source external software package CasADi [1]. The OCP was solved with IPOPT [23]. Then the scenario-based deterministic equivalent of Equation 2.37 can be formulated as:

$$\min_{x,z,u} \quad \mathbb{E} \sum_{l=1}^{S} \sum_{k=1}^{N} \Big(- \frac{\dot{m}_{gas}(\mathbf{x}, \mathbf{z}, \mathbf{u}, \mathbf{p})}{(1+i)^t} \Big). \tag{2.38}$$

Constraints are imposed on the following variables:

$$\begin{aligned} 0.75 \ &\leq \ u_{\text{comp}} \ \leq \ 1.05 \\ 0 \ &\leq \ u_{\text{choke}} \ \leq \ 1 \\ 0 \ &\leq \ X \leq \ \epsilon_r \\ 0 \ &\leq Srg \\ 0 \ &\leq Stw \\ 150 \text{ bar} \ &\leq P_{\text{out}} \\ x(0) \ &= x_0. \end{aligned} \tag{2.39}$$

Health condition constraints are expressed as X where ϵ_r is the upper bound for the reliability objective. Other constraints are enforced on inputs, u_{comp} and u_{choke}, related to allowable operating range for flow through compressor and choke. Constraints on surge, Srg, and Stonewall, Stw, conditions for compressor choking according to the allowable operating range must be imposed. Constraint on P_{out} is necessary to ensure flow trough the pipeline to topside. Initial condition is the last equality constraint [22].

Chapter 3

Results and Discussion

This chapter presents the results obtained working with this project thesis. A thorough analysis of the derived separator model and optimal open-loop solutions for the health prognostics models is given in this chapter. At the end, the degradation of equipment will be compared to remaining useful life (RUL) of equipment for this subsea system.

3.1 Overview

The overall objective is to maximize the NPV of production without jeopardizing the reliability of the subsea system. Health prognostics models are included in the optimization. This gives a MPC-like framework in which constraints are imposed on the allowable degradation of the equipment and on the RUL of the equipment. Essentially, this refers to ensuring that the subsea system stays operational until the next maintenance intervention. In the context of this work, the next maintenance engagement is scheduled to take place five years after the start-up of the plant. However, the simulation is conducted with t_f = 1 as a simplification in the calculations. The simulation was carried out with a fixed compressor strain on the bearing fault in the wet-gas compressor. The initial bearing crack length was set to 0.01 mm at t = 0.

A scenario-based method is employed to account for the uncertainty in the c_{Paris} parameter in the bearing crack propagation model in Equation 2.21. The scenarios represent discrete parameter realizations, that is the 90% percentile, the 10% percentile, and the nominal value. The stochastic optimal control problem (OCP) expressed in Equations 2.38 - 2.39 is solved with initial prediction horizon N = 20 and a robust horizon of N_R = 1 for the the scenario tree. A current optimal control trajectory is computed with process disturbance being conditionally dependent of previous disturbances. This is the optimal

open-loop solution which will be discussed in later sections.

3.2 Implementation in MATLAB

Equations for the separator model and RUL of equipment calculations are used to modify the original system implemented in MATLAB by Adriaen Verheyleweghen. Equations are stated as algebraic or differential equations and added in the already existing system. The resulting MATLAB code is provided in a zip-file.

3.3 Separator model

A detailed model enables us to accurately predict liquid carry over to the wet-gas compressor. The purpose of the new separator model is to reduce uncertainty and enable enhanced production through less conservative operations. The new separator model aims to try to replicate the separator in the Åsgard subsea gas compression station. Needed equations for modelling the separator were found in Section 2.3.1. Simplifications have been necessary to incorporate this model in the already existing system in MATLAB developed by Adriaen Verheyleweghen. The following assumptions are inspired by the developer of the model [3]:

- Volumetric liquid flow, $\dot{Q}_l$, entering the separator is approximately constant and 10% of the volumetric gas flow, $\dot{Q}_g$.
- Tangential gas velocity at the cyclone wall is assumed to be constant and equal to 3.75 m/s.
- The angle in Figure 2.5, $\hat{\theta}$, is assumed to be constant and equal to = 45^o.
- θ is the angle for the tangential gas velocity at the cyclone wall. This is assumed to be constant and equal to 45^o.
- Liquid dynamic viscosity of fluid, μ_l, is assumed to be constant and equal to 0.096 cP at inlet pressure 100 bar.
- Interfacial tension between the two phases is assumed to be constant and equal to 2.2 mN/m at inlet pressure 100 bar.
- Liquid film is in the transition of the Reynolds number. K and m for the friction factor for liquid on the cyclone wall are constant and equal to 1.926 and -1/3 respectively.

- Model parameter a is assumed constant and set to 0.4.
- The linearization parameters, A and B, are modeled as -0.1345 and 1.01, respectively.

These are rough approximations for a separation unit in which the inlet flow predominantly contains gas. In reality, the separator should be able to handle various GVFs and tangential gas velocities. The physical properties of the gas and liquid phase will also vary. This should be addressed in future work.

Implementing the new separator model generates some interesting relations. Figure 3.1a illustrates how separation efficiency decreases with superficial gas velocity. This plot shows the same trend as Figure 2.3 for the Statoil patent. However, the relative separation efficiencies are hard to compare as operating conditions may differ. Figure 3.1b illustrates how separation efficiency decreases with increasing re-entrainment number according to this separator model.

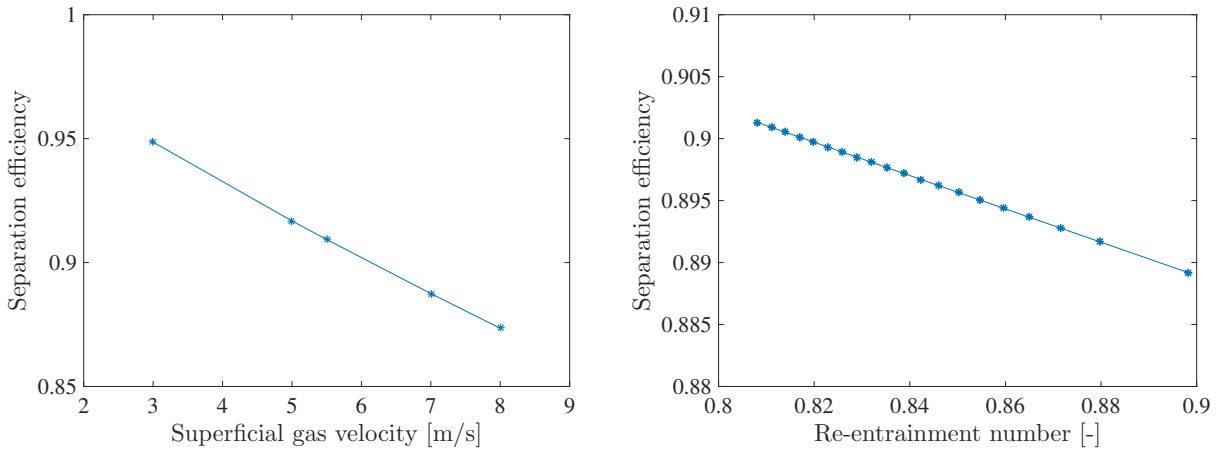

(a) Separation efficiency as a function of Superficial gas velocity. (b) Separation efficiency as a function of Re-entrainment number.

Figure 3.1: Separation efficiency for the new separator model as a function of Superficial as velocity and Re-entrainment number.

The model constant a from Equation 2.18 and regression parameters, A and B, in Equation 2.19 , result in a good fit between the re-entrainment number, E, and the separation efficiency, α, for the separator. This correlation gives an indication that the separation efficiency is dominated by re-entrainment of liquid from the gas stream, rather than insufficient separation of droplets.

Based on the calculated Reynolds number for the liquid film on the cyclone wall, Re_L, all simulations were within the transition regime. The constants, K and m in Section 2.3.1 were selected accordingly.

The dimensionless viscosity number, N_μ, were less than 1/15 for all simulations as well. Thus, the assumptions in Section 2.3.1 were credible for the dimensionless re-entrainment number, E.

3.4 Parameter estimation

The derivation of the cumulative hazard function in Section 2.4.1 introduces some parameters, the scale parameter, λ_w, and the shape parameter, k_w. At first, let us evaluate the properties and significance of these parameters. The shape parameter k_w and the scale parameter λ_w were introduced in Equation 3.2. Assumptions were made that both shape and scale parameters were dependent on the degradation variable, h. However, it appeared to be difficult to find an optimal solution with the shape parameter depending on the system degradation. Based on support from [16], models describing failure due to mechanical stress can assume a constant shape parameter. Further simulations were run with constant shape parameter and a scale parameter that is dependent on h.

The characteristics of the scale and shape parameters are key in investigating the RUL distribution of the system. Different shape parameters affect the failure rate in the following manner [9]:

1. $k_w < 1$ Suitable for modelling early failure due to problems with production
2. $k_w = 0$ Suitable for modelling failure due to pure coincidence
3. $k_w > 1$ Suitable for modelling wear-out failure due to degradation of equipment after some time

The shape parameter represents the slope of the Weibull distribution and in the context of this work, it is appropriate to use a positive shape parameter. The failures occurring are assumed to be "wear-out"-failures. Failures will commence due to "the aging process". Hence the failure rate $h_{RUL}(t)$ ought to increase with time. The scale parameter represents the variance of the Weibull distribution. The scale parameter was assumed to be greater than zero as it is inversely proportional to the Weibull PDF in Equation 2.23. It is assumed to decrease over time since RUL distribution has a greater variance earlier in the production. Due to the lack of failure data, the final relationship between the shape, k_w, and scale, λ_w, parameter and the crack length, h, is assumed to be:

$$k_w = 3 \tag{3.1}$$

$$\lambda_w = 1.2 - h \tag{3.2}$$

In real systems, the parameter values must be adjusted to reflect the expected degradation profile of the given system. Historical data from the OREDA database or similar can be used for this purpose [13].

3.5 Optimal open-loop solution

The optimal control problem (OPC) in Equation 2.38 and 2.39 is investigated using two propagation models for health condition monitoring. The first case is conducted by imposing constraints on the maximum allowable degradation of the bearing crack length in the wet-gas compressor. Degradation of equipment is estimated from the bearing crack-length in the wet-gas compressor, which will degrade according to Paris' law of crack propagation. The second case is solved by imposing constraints on the maximum allowable cumulative hazard. The RUL of equipment is measured as risk of failure associated with the whole production strategy from t=0 to t=t_f. This risk is captured by the cumulative hazard, $H_{RUL}(t_f)$.

3.5.1 Constrained bearing crack length

Degradation of equipment is measured as bearing crack-length in the wet-gas compressor, which will degrade according to Paris' law of crack propagation. The evolution of the bearing crack-length, h, over time is illustrated in Figure 3.2a. Constraints are imposed on h to ensure that the wet-gas compressor stays operational until the next maintenance intervention. The degradation threshold is set to h = 1 mm.

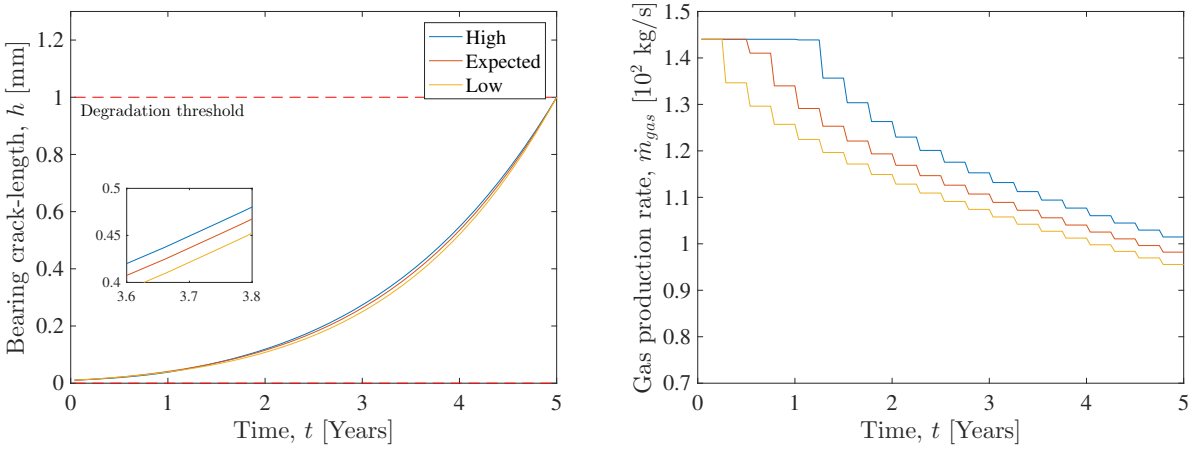

(a) Bearing crack-length, h, as a function of time , t.

(b) Gas production rate, $\dot{m}_{gas}$, as a function of time, t.

Figure 3.2: State profiles for bearing crack length, h, and gas production rate, $\dot{m}_{gas}$. Health condition is measured in terms of system degradation.

Figure 3.2b indicates that the gas production rate decreases with time. This is reasonable as the NPV concept in the objective function in Equation 2.38 favours early gas production rather then late production. A section of the plot in Figure 3.2a provides insight into how the uncertain parameter c_{Paris}, affects the crack propagation model. The crack length is greater with higher values of the uncertain parameter, c_{Paris}. This is logical as this parameter is directly proportional to the derivative of the crack-length. The scenario-based approach ensures robustness to disturbance and uncertainty given reasonable, discrete parameter realizations. More parameters could be modeled with uncertainty, but that would demand more computational time. The disturbance in GVF should be handled in future work to be able to account for fluctuations in the gas volume fractions in the system.

The hazard function, $h_{RUL}(t)$, is given in Equation 2.28 and is plotted in Figure 3.3a. Risk associated with overall production strategy from t = 0 to t = t_f is expressed in the cumulative hazard function, $H_{RUL}(t_f)$. $H_{RUL}(t_f)$ is illustrated in Figure3.3b.

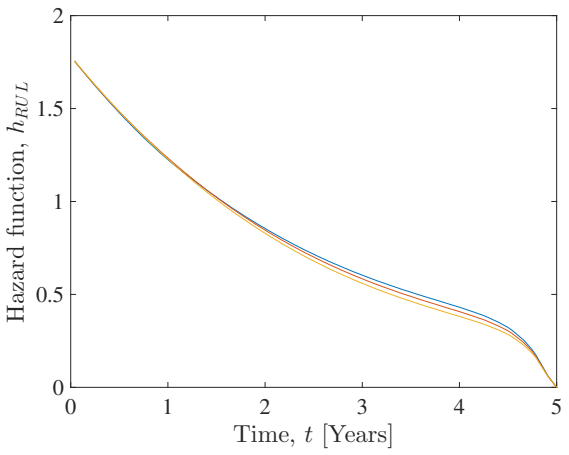

(a) Hazard function, $h_{RUL}(t)$, as a function of time, t.

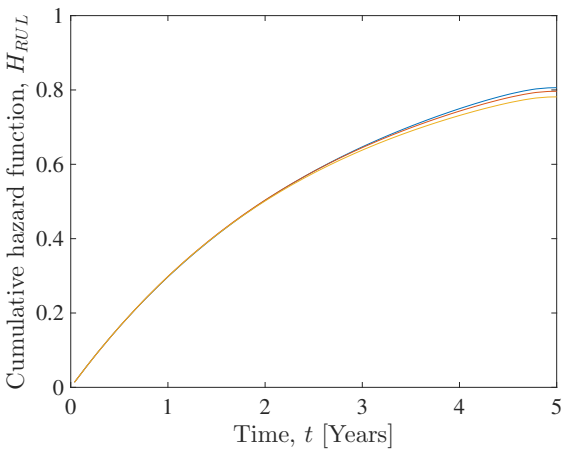

(b) Cumulative hazard function, $H_{RUL}(t_f)$, as a function of time, t.

Figure 3.3: Risk of failure for the system when degradation of the bearing crack-length, h, is used as health propagation model.

As this is conditional probability in an "aging" process, the failures occurring are assumed to be "wear-out"-failures. Hence the failure rate $h_{RUL}(t)$ ought to increase with time. Figure 3.3a illustrates a decreasing failure rate with respect to time. The plot in Figure 2.28 indicates a contradicting result which is likely to be the reverse of the h_{RUL} estimates. This is because the implementation of h_{RUL} and H_{RUL} was conducted by introducing a new differential time variable. The cumulative risk, H_{RUL}, would thus be slower if it was solved properly. In future work, the time dependency in h_{RUL} and H_{RUL} should be embedded

without introducing a new time variable.

3.5.2 Constrained cumulative risk

The health condition of the overall system is also evaluated when it is measured in terms of RUL of equipment. Constraints are imposed on the cumulative hazard, $H_{RUL}(t_t)$, to assure safe and reliable operation. The cumulative hazard threshold is based on maximum cumulative hazard obtained in Section 3.5.1 and is set to $H_{RUL}(t_t) = 0.8061$. Figure 3.4 illustrates the predicted RUL of equipment when constraints are imposed on the cumulative hazard.

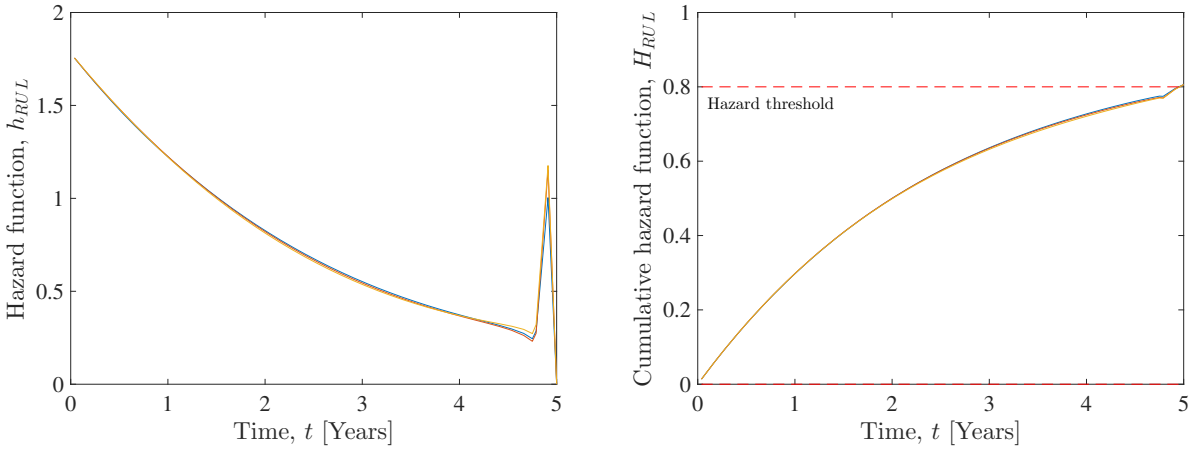

(a) Hazard function, $h_{RUL}(t)$, as a function of time, t.

(b) Cumulative hazard function, $H_{RUL}(t_f)$, as a function of time, t.

Figure 3.4: Risk of failure for the system when cumulative hazard, $H_{RUL}(t_f)$, is used to make health predictions.

There is a significant increase in the hazard function in Figure 3.4a. There is also a small notch in the cumulative hazard in Figure 3.4b. This increase is also significant in the state profiles for the gas production rate, $\dot{m}_{gas}$, and the bearing crack length, h, in Figure 3.5. Towards the end of the time horizon, the system realizes that the health constraint will be met, and thus increases the inputs to squeeze more gas production out of the system. This indicates that the specified maintenance horizon might have been too short. Preferably, the next maintenance should have been planned later. This might be avoided if the h_{RUL} and H_{RUL} was implemented without introducing a new differential time variable. The shape and the scale parameters discussed in Section 3.4 were equal for both prognostics models. However, different tunings of the parameters did not remove the notch in the state profiles.

The predicted development of the bearing crack-length in the wet-gas compressor is illustrated in Figure

3.5a. The bearing crack-length is not used for health predictions for the system in this case and is therefore not constrained. The bearing crack-length is predicted to reach a maximum value of h = 1.254 mm after 5 years. The development of the associated gas production rate, $\dot{m}_{gas}$, is illustrated in Figure 3.5b. The gas production rate in Figure 3.2b and 3.5b is not significantly different, despite the notch at the very end in the latter figure. Therefore, the result of the objective function ought to be rather similar.

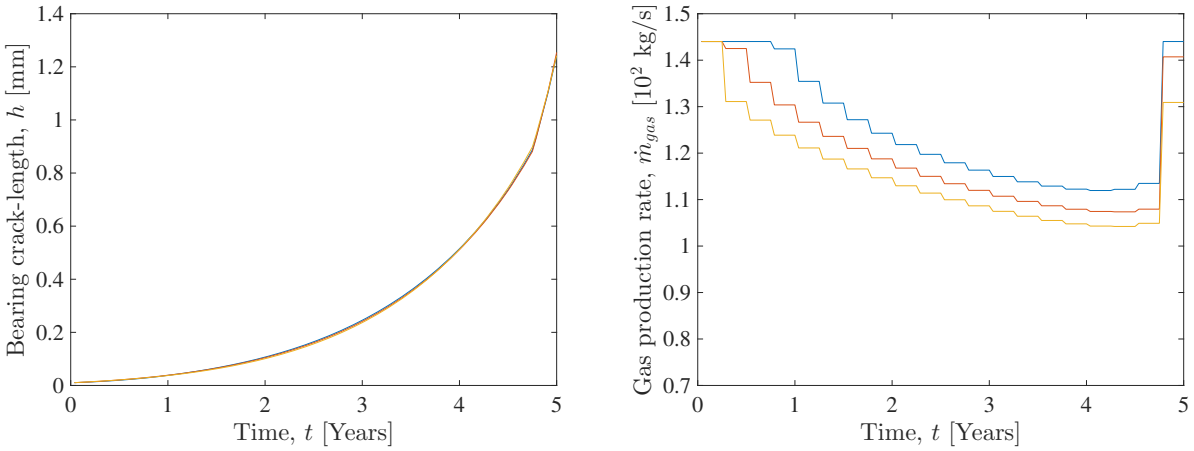

(a) Bearing crack-length, h, in the wet-gas compressor as a function of time, when the health condition is measured in terms of RUL of equipment.

(b) Gas production rate, $\dot{m}_{gas}$, as a function of time, t.

Figure 3.5: State profiles for the bearing crack length, h, in the wet-gas compressor and the gas production rate, $\dot{m}_{gas}$. Health condition is measured in terms of RUL of equipment.

3.5.3 Degradation level and RUL-distribution

The risk captured by the hazard function, H_{RUL}, can be directly affected by shaping the RUL-distribution. The RUL-distribution can be formed by influencing the states x by adjusting the inputs u. Figure 3.6b and 3.7b shows the evolution of the degradation of the bearing crack length, h, over a time period of 5 years. The corresponding RUL distribution at degradation levels h_1, h_2 and h_3 are depicted in Figure 3.6a and 3.7a. Essentially the expected RUL increases with decreasing degradation. That is reasonable as a smaller bearing crack-length would suggest that the system is operational for a longer time, compared to a larger crack-length.

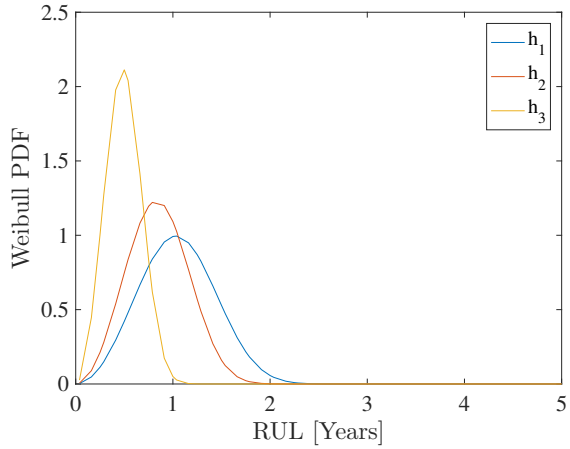

(a) RUL distribution at degradation levels h_1, h_2 and h_3.

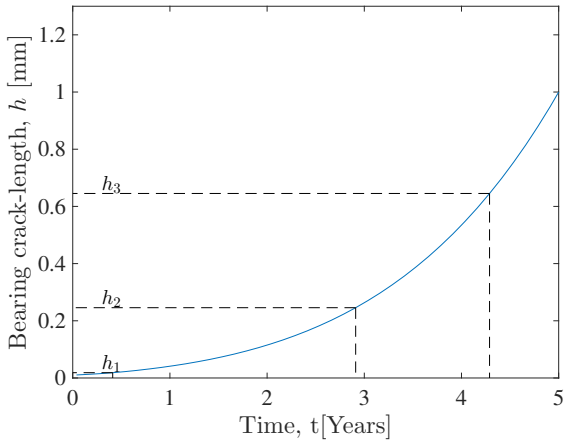

(b) Bearing crack length at three stages of the degradation development, h_1, h_2 and h_3.

Figure 3.6: Evolution of the degradation of equipment, h, and the RUL- distributions at degradation levels h_1, h_2 and h_3. Degradation of equipment is used to make health predictions.

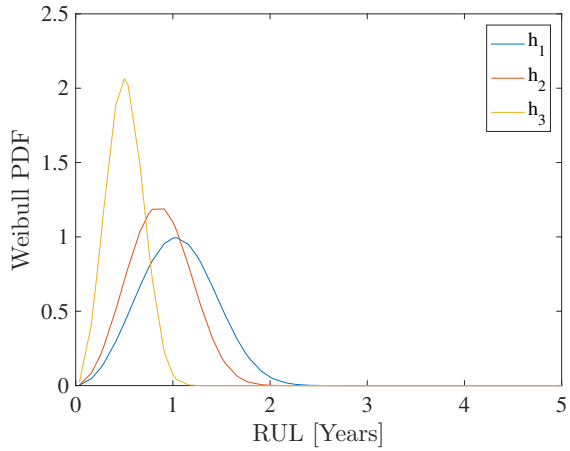

(a) RUL distribution at degradation levels h_1, h_2 and h_3.

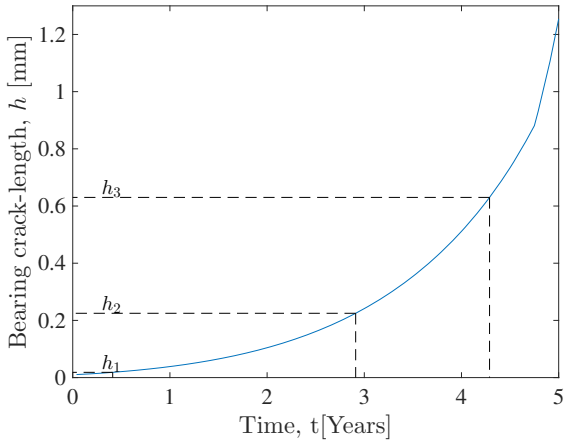

(b) Bearing crack length at three stages of the degradation development, h_1, h_2 and h_3.

Figure 3.7: Evolution of the degradation of equipment, h, and the RUL- distributions at degradation levels h_1, h_2 and h_3. Cumulative hazard is used to make health predictions.

Table 3.1 shows the results from the open-loop optimization for the two health propagation models. Overall, the results are somewhat unexpected. The gas production from the two health propagation models is quite similar. Based on a rational mindset, the degradation of equipment as a health propagation model ought to yield a more economically profitable operation as it imposes constraints directly on the fault indicator. RUL of equipment as a health propagation model would suggest a more conservative operational strategy as it seeks to limit loss of production. The economic outcome is reflected in Figure 3.2b

and 3.5b, in which the gas production with a notch at the end would yield a more profitable operational strategy. The outcome might be more intuitive if h_{RUL} and H_{RUL} were embedded without introducing a new differential time variable.

Table 3.1: Bearing crack length,h and cumulative hazard,$H_{RUL}(t_f)$, for the two health propagation models.

Health propagation model	Bearing crack length, h	Cumulative hazard, $H_{RUL}(t_f)$	Gas production, $\dot{m}_{gas}$
Degradation of equipment	0.8061	1.0	2.46867
RUL of equipment	0.8061	1.254	2.49838

Chapter 4

Conclusion

This project thesis proposed an approach for integrating health monitoring, prognostics and control to achieve an economic optimal operational strategy, without compromising the reliability of the system. A detailed model has been implemented to provide accurate predictions of liquid carry over to the wet-gas compressor. The purpose of the new separator model has been to reduce uncertainty and enable enhanced production through less conservative operations. Excellent correlation between the cyclone separation efficiency and the dimensionless re-entrainment number indicated that the separation efficiency was governed by liquid re-entrainment, i.e. not insufficient separation of smaller droplets.

Health monitoring techniques has been employed to consider and evaluate the condition of the overall system. The degradation of equipment and remaining useful life (RUL) of equipment has been used for condition monitoring purposes. Paris' law for crack propagation has been used to predict degradation of equipment. Risk of failure in terms of cumulative hazard has been used to predict RUL of equipment. Parameters in the RUL distribution has been estimated based on the aging process. The expected RUL increases with decreasing degradation. That is reasonable as a smaller bearing crack-length would suggest that the system was operational for a longer time, compared to a larger crack-length. The results of the economic outcome are somewhat unexpected. The RUL of equipment as a health propagation model seems to be more profitable. Adjustments to the risk of failure implementation could have been made to achieve a more intuitive result.

4.1 Future Work

In future work, a separator model with a spinlet inlet configuration can be considered. Thus the model would capture more features of the original Statoil patent for the subsea station. More parameters could be modeled with uncertainty, but that would demand more computational time. The disturbance in GVF should be handled in future work to be able to account for fluctuations in the gas volume fractions in the system.

The implementation of risk of failure ought to be conducted without introducing a new differential time variable in order to avoid confusion. An increasing failure rate for the aging process is more intuitive and might prevent the notch at the end. Multiple failure mechanisms should also be addressed in the future, not only the faults which can be affect by inputs. Furthermore, the objective can be changed to be minimizing the unavailability whilst constraining the minimum expected economic profit. This indicates that the objective is to minimize the cumulative risk of failure while constraining the minimum expected economic profit from operation. This can be expressed as:

$$\begin{aligned} \min_{u} \quad & (\bar{\phi}_r(x,z,u,p)) \\ \text{s.t.} \quad & x \in X \\ & u \in U \\ & \bar{\phi}_e(x,z,u,p) \leq \epsilon_e \end{aligned} \tag{4.1}$$

Bibliography

[1] Andersson, J. (2013). *A General-Purpose Software Framework for Dynamic Optimization*. Ph.D. thesis, Arenberg Doctoral School, KU Leuven, Department of Electrical Engineering (ESAT/SCD) and Optimization in Engineering Center, Kasteelpark Arenberg 10, 3001-Heverlee, Belgium

[2] Aguilera, L.C.P. (2013). *Subsea Wet Gas Compressor Dynamics*. Master thesis, Norwegian University of Science and Technology.

[3] Austrheim, T. (2006). *Experimental Characterization of High-pressure Natural Gas Scrubbers*. Ph.D. thesis, University of Bergen.

[4] Bechhoefer, E., Bernhard, A., and He, D. (2008). *Use of paris law for prediction of component remaining life*. In Aerospace Conference, 2008 IEEE, 1–9. IEEE.

[5] Diehl, M. (2011). *Numerical optimal control*. Optimization in Engineering Center (OPTEC).

[6] Fredheim, A.O., Gjertsen, L.H., Rusten, B.H., Austrheim, T. and Johnsen, C.G. (2011) *Google patents: Separator Unit*. US Patent App. 12/866,285 http://www.google.com/patents/US20110016835.

[7] Hans,C., A.,Sopasakis,P., Bemporad, A., Raisch, J. and Reincke-Collon, C. (2015). *Scenario-Based Model Predictive Operation Control of Islanded Microgrids*. 2015 IEEE 54th Annual Conference on Decision and Control (CDC).

[8] Institute of Electrical and Electronics Engineers. (1990). *IEEE Standard Computer Dictionary: A Compilation of IEEE Standard Computer Glossaries*. New York, NY ISBN 1-55937-079-3.

[9] Jiang, R., Murthy, D.N.P. (2011). *A study of Weibull shape parameter: Properties and significance*. Reliability Engineering System Safety. 96 (12): 1619–26.

[10] Kleinbaum, D. G. and Klein. M. (1996). *Survival analysis: a self-learning text*. New York, Springer.

[11] Kurt, Daniel (2003-11-24). *Net Present Value (NPV) Definition | Investopedia*. Investopedia. Retrieved 2017-12-05.

[12] Lucia, S., Subramanian, S., and Engell, S. (2013b). *Non-conservative robust nonlinear model predictive control via scenario decomposition*. In Control Applications (CCA), 2013 IEEE International Conference on, 586–591. IEEE.

[13] OREDA database. https://www.oreda.com/database/.

[14] Paris, P. and Erdogan, F. (1963). *A critical analysis of crack propagation laws. Journal of basic engineering*, 85(4), 528–533.

[15] Pereira, E.B., Galvao, R.K.H., and Yoneyama, T. (2010). *Model Predictive Control using Prognosis and Health Monitoring of actuators*. In Industrial Electronics (ISIE), 2010 IEEE International Symposium on, 237–243. IEEE.

[16] Pham, H. (2003). *Handbook of Reliability Engineering*. New York, Springer p 451.

[17] Seborg, D. E., Edgar, T. F., Mellichamp, D. A. and Doyle, F. J. (2010). *Process dynamics and control*. 2010. Hoboken, N.J.. Wiley.

[18] Setekleiv, E., Anfray, J., Boireau, C., Gyllenhammar, E. and Kolbu, J. (2016). *An Evaluation of Subsea Gas Scrubbing at Extreme Pressures*. 10.4043/27154-MS.

[19] Verheyleweghen, A. (2017). *Defining the objective and reliability constraints*. Manuscript in preparation, Norwegian University of Science and Technology.

[20] Verheyleweghen, A. (2017). *Framework for Combined Diagnostics, Prognostics and Optimal Operation of a Subsea Gas Compression Station*. Paper, Norwegian University of Science and Technology.

[21] Verheyleweghen, A. (2016). *Health Estimation and Optimal Operation of a Subsea Gas Compression System Under Uncertainty*. Power point, Norwegian University of Science and Technology.

[22] Verheyleweghen, A. (2017). *Health Estimation and Optimal Operation of a Subsea Gas Compression System Under Uncertainty*. Paper, Norwegian University of Science and Technology.

[23] Wachter, A. and Biegler, L.T. (2006). *On the implementation of an interior-point filter line-search algorithm for large-scale nonlinear programming*. Mathematical programming, 106(1), 25–57.

Appendix A

Parameters used for the simulations

Table A.1: Parameters used for the simulations.

Parameter	Description	Value	Unit
m	Model parameter for the Re-entrainment number,E.	0.4	-
A	Linearization parameters for the correlation between E and α.	-0.1345	-
B	Linearization parameters for the correlation between E and α.	1.01	-
θ	Angle between vertical and tangential gas velocity on the cyclone wall.	45	^{o}
$\hat{\theta}$	Angle to indicate direction of gas flow in the wetted perimeter.	45	^{o}
σ	Interfacial/surface tension between two phases.	2.2	mN/m
μ_l	Liquid viscosity.	0.096	cP
P_1	Inlet pressure.	100	bar
u_{choke}	Choke opening.	0.565	-
u_{comp}	Compressor speed.	0.85	-
T	Inlet temperature.	350	K
h_0	Initial bearing degradation.	0.01	mm
i	Discount rate for Net present value calculations.	0.015	-
N	The length of the horizon in the stochastic non-linear optimization problem.	20	-